International Journal of Fluid Mechanics Research, Vol. 27, Nos. 2–4, 2000

Boundary Layer Flow of a Fluid-Particle Suspension Past a Flat Plate in the Presence of a Magnetic Field

A. J. Chamkha[1] and **J. Peddieson**[2], **Jr.**
[1]Department of Mechanical and Industrial Engineering, Kuwait University
Safat, Kuwait
[2]Department of Mechanical Engineering, Tennessee Technological University
Cookeville, Tennessee, U.S.A.

The plane, steady, laminar, boundary-layer flow of a two-phase fluid/particle suspension in the presence of a variable transverse magnetic field is simulated using an extension of the dusty-gas model which includes dispersed-phase diffusivity and viscosity. Numerical calculations based on this model show that its predictions are quite different from those of the dusty-gas model.

* * *

Introduction

This study is concerned with mathematical modeling of plane, steady, laminar, boundary-layer flow of a particulate suspension past a semi-infinite flat plate in the presence of a variable transverse magnetic field. This is a fundamental problem in fluid-particle mechanics which has not been solved. In addition, hydromagnetic boundary-layer flow has several technological and engineering applications such as design of heat exchangers, cooling of nuclear reactors, geothermal reservoirs, flow meters, flight control of an aircraft or a space vehicle, and final product quality control of some metallurgical processes. Studies on hydromagnetic boundary-layer flow over flat plates with transverse non-moving magnetic fields demonstrate that the magnetic field reduces the skin friction and heat transfer. They can also be used to determine the losses at flat or nearly flat surfaces such as thin airfoils and the side walls of large volume magnetohydrodynamic generators and accelerators. The MagnetoFluid-Dynamic (MFD) phenomena result from the mutual effect of a magnetic field and a conducting fluid flowing across it. Thus, a flow resistive (if magnetic field is non-moving) or pumping (if magnetic field is moving with the fluid) force is produced in the fluid (see Cramer and Pai [1]). During the past decade or so, Osiptsov [2], Prabha and Jain [3], Wang and Glass [4] Chamkha and Peddison [5] and Chamkha [6] and [7] have reported numerical solutions for laminar flow of a particulate suspension past a flat plate in the absence of a magnetic field. (The paper by Wang and Glass [4] is, incidentally, a good source of references dealing with earlier series expansion and momentum integral approaches to the problem). In the first three studies, it was assumed that the volume fraction of particulate material was small, that the particle phase was stress free, and that no particle-phase diffusive effects existed. The model produced by these assumptions will

ISSN 1064-2277

herein be called the dusty-gas model after Marble [8]. Particulate-phase stresses and/or diffusive effects have been considered by Chamkha and Peddieson [5] and Chamkha [6] and [7]. Osiptsov [2], Prabha and Jain [3] and Chamkha and Peddieson [5] assumed fluid incompressibility while Wang and Glass [4] and Chamkha [6] and [7] considered fluid compressibility. In situations, such as those mentioned earlier, where the fluid is electrically conducting and a magnetic field is present, the flow dynamics of the particulate suspension are modified. Therefore, the effects of the magnetic field must be taken into account in the two-phase flow model.

An early study of an electrically-conducting fluid flow over a semi-infinite flat plate in the presence of a transverse magnetic field both fixed to the surface and fixed to the main flow was reported by Rossow [9]. He obtained series solutions of the problem for both moving and non-moving magnetic fields. The book by Cramer and Pai [1] contains more related references and information on the subject.

The dusty-gas model has been widely used. It is, however, certainly not the only plausible model of the behavior of small volume fraction fluid/particle suspensions. It is, therefore, of interest to obtain solutions to flow problems using other models and compare their features to those of the corresponding dusty-gas solutions. The information obtained in this way should facilitate the matching of models with observed physical behavior. In the work to be described herein, the problem of steady, laminar, hydromagnetic, boundary-layer flow of a particulate suspension past a flat plate is solved employing a model which retains the small volume fraction assumption but includes particle-phase viscous and diffusive effects and fluid-phase hydromagnetic effects. The model incorporates ideas that are similar to those to be found in the book and papers of Soo [10], [11], and [12] and Chen and various coworkers (see, for instance, Korjack and Chen [13]). The fluid phase is assumed Newtonian and electrically conducting while the particle phase is assumed pressureless and electrically non-conducting. The magnetic Reynolds number is assumed to be small so that the induced magnetic field is neglected. Also, no electric field is assumed to exist and the Hall effect of magnetohydrodynamics is neglected.

In the remainder of this paper, the governing equations associated with the model discussed above are formulated and representative numerical solutions of these equations are presented graphically. It is shown that the present model is capable of predicting results which are quite different from those reported in [2] and [3] in the absence of fluid-phase magnetic field effects.

Problem Formulation

Consider the steady, laminar, boundary-layer flow of a particulate suspension past a semi-infinite flat plate occupying the half of the x, z plane corresponding to $x \geq 0$, with the y axis being normal to the plate. A magnetic field with variable strength $B(x) = B_0/x^{1/2}$ (where B_0 is a constant) is applied in the y direction normal to the flow direction. Variable applied magnetic fields have been used by previous investigators such as Chiam [14] in his work on hydromagnetic flow over a continuously stretched surface. Far from the plate, the free stream is characterized by a constant velocity u_∞ in the positive x direction and a constant in-suspension particle-phase density $\rho_{d\infty}$ (see Fig. 1). Let ρ_c, u_c, v_c, ν_c and σ_c denote the fluid-phase (continuous-phase) in-suspension density, tangential velocity, normal velocity, kinematic viscosity and electrical conductivity, respectively. Let ρ_d, u_d, v_d, ν_d, and D_d denote the particulate-phase (dispersed-phase) in-suspension density, tangential velocity, normal velocity, kinematic viscosity, and diffusivity, respectively. Finally, let τ denote the momentum relaxation time of the suspension (see, for instance, Marble [8]). In terms of this notation, the partial differential equations which form the basis for the present work can be written as

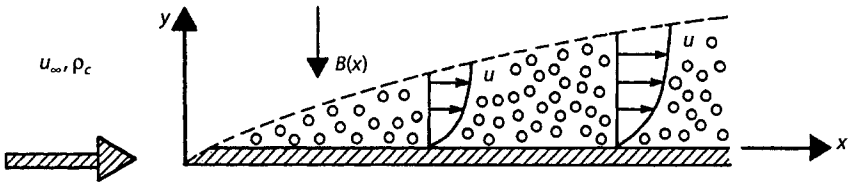

Fig. 1. Geometry and coordinate system.

$$\partial_x u_c + \partial_y v_c = 0$$

$$u_c \partial_x u_c + v_c \partial_y u_c = \nu_c \partial_{yy} u_c + \left(\frac{\rho_d}{\rho_c}\right)(u_d - u_c)/\tau - \sigma_c B^2 (u_c - u_\infty)/\rho_c$$

$$\partial_x(\rho_d u_d) + \partial_y(\rho_d v_d) = D_d \partial_{yy} \rho_d$$

$$u_d \partial_x u_d + v_d \partial_y u_d = \nu_d(\partial_{yy} u_d + \partial_y(\ln \rho_d)\partial_y u_d) + (u_c - u_d)/\tau$$

$$u_d \partial_x v_d + v_d \partial_y v_d = \nu_d(2(d_{yy} v_d + \partial_y(\ln \rho_d)\partial_y v_d) + \partial_{xy} u_d + \partial_x(\ln \rho_d)\partial_y u_d) + (v_c - v_d)/\tau \qquad \text{(1a–e)}$$

In writing the above equations, the usual boundary-layer approximations were employed, external body forces other than the magnetic force were neglected, and, for simplicity, the quantities ρ_c, ν_c, σ_c, ν_d, D_d, and τ were treated as constants. In should be mentioned that since the magnetic Reynolds number is assumed to be small. Maxwell's equations are uncoupled from the boundary-layer equations. The equations employed by Osiptsov [2] and Prabha and Jain [3] are recovered by equating D_d to zero in Eq. (1c) and ν_d to zero in Eqs. (1d, e). The terms multiplied by D_d and ν_d may be thought of as logical consequences of the averaging processes used to develop a continuum model of a system containing discrete elements. They recognize the possibility that the properties at a typical point in a small volume element may differ somewhat from the corresponding averages over the volume element. Such differences give rise to fluxes of mass and linear momentum not accounted for by the averaged variables.

Depending on the way in which the averaging process is carried out, additional mass balances for both phases (see, for instance, Soo [12]), one phase (see, for instance, Buyevich [15]), or neither phase (see, for instance. Drew [16]). A recent paper in which the inclusion of such terms had a beneficial effect on solution properties is that by Ungarish and Greenspan [17]. In the present work, it is assumed that a term of this kind appears in the particle-phase mass balance (1c) and that it is modeled by a diffusive mechanism (following Soo [10] and [12]). Similarly, it is assumed that additional linear momentum fluxes appear in the particle-phase linear momentum balances Eqs. (1d, e) and that they are modeled by viscous mechanisms (following Soo [11] and Korjack and Chen [13]). In these investigations ([11] and [13]), it was assumed that $\nu_d = D_d$. This assumption was not employed herein so as to permit the separate investigation of particulate diffusive and viscous effects.

It should be pointed out that Eq. (1c), as it stands, is not the usual convection/diffusion equation (because u_d and v_d, rather than u_c and v_c, appear therein). The convection/diffusion limit is reached when the interphase drag terms dominate in Eqs. (1d, e). Then these equations read,

respectively $u_d = u_c$ and $v_d = v_c$. Substitution of those expressions into Eq. (1c) produces the normal convection/diffusion formulation.

It was felt to be convenient to employ the modified Blasius transformations

$$x = \frac{u_\infty \tau \xi}{1-\xi} \qquad y = \left(\frac{2\nu_c \tau \xi}{1-\xi}\right)^{1/2} \eta$$

$$u_c = u_\infty F_c(\xi, \eta) \qquad v_c = \left(\frac{\nu_c(1-\xi)}{2\tau\xi}\right)^{1/2} (G_c(\xi, \eta) + \eta F_c(\xi, \eta))$$

$$u_d = u_\infty F_d(\xi, \eta) \qquad v_d = \left(\frac{\nu_c(1-\xi)}{2\tau\xi}\right)^{1/2} (G_d(\xi, \eta) + \eta F_d(\xi, \eta))$$

$$\rho_d = \rho_{d\infty} Q_d(\xi, \eta) \tag{2}$$

Substituting Eqs. (2) into Eqs. (1) yields

$$\partial_\eta G_c + F_c + 2\xi(1-\xi)\partial_\xi F_c = 0$$

$$G_c \partial_\eta F_c + 2\xi(1-\xi) F_c \partial_\xi F_c = \partial_{\eta\eta} F_c - 2\mathrm{Ha}^2(F_c - 1) + 2\kappa\xi Q_d(F_d - F_c)/(1-\xi)$$

$$G_d \partial_\eta Q_d + 2\xi(1-\xi) F_d \partial_\xi Q_d + (\partial_\eta G_d + F_d + 2\xi(1-\xi)\partial_\xi F_d) Q_d = \delta \partial_{\eta\eta} Q_d$$

$$G_d \partial_\eta F_d + 2\xi(1-\xi) F_d \partial_\xi F_d = \beta(\partial_{\eta\eta} F_d + \partial_\eta(\ln Q_d)\partial_\eta F_d) + 2\xi(F_c - F_d)/(1-\xi)$$

$$G_d \partial_\eta G_d + 2\xi(1-\xi) F_d \partial_\xi G_d - \eta F_d^2 = \beta(2(\partial_{\eta\eta} G_d + \partial_\eta(\ln Q_d)\partial_\eta G_d) + 3\partial_\eta F_d + \partial_\eta(\ln Q_d) F_d + 2\xi(1-\xi)(\partial_{\xi\eta} F_d + \partial_\xi(\ln Q_d)\partial_\eta F_d)) + 2\xi(G_c - G_d)/(1-\xi) \tag{3a–e}$$

where

$$\beta = \frac{\nu_d}{\nu_c} \qquad \delta = \frac{D_d}{\nu_c} \qquad \kappa = \frac{\rho_{d\infty}}{\rho_c} \qquad \mathrm{Ha}^2 = \frac{\sigma_c B_0^2 \tau}{\rho_c} \tag{4}$$

are the viscosity ratio, the inverse Schmidt number, the free stream particle loading and the square of the Hartmann number, respectively. It is worth noting that if the magnetic field is uniform, use of Eqs. (2) produces a singular behavior at $\xi = 1$ where the fluid velocity profile has an infinite slope at the plate surface. However, the use of a magnetic field which varies inversely with x eliminates this problem.

Equations (3) are supplemented by the boundary conditions

$$F_c(\xi, \eta) \to 1 \qquad F_d(\xi, \eta) \to 1 \qquad Q_d(\xi, \eta) \to 1 \quad \text{as} \quad \eta \to \infty$$

$$G_d(\xi, \eta) \to G_c(\xi, \eta) \quad \text{as} \quad \eta \to \infty$$

$$F_c(\xi, 0) = 0 \qquad G_c(\xi, 0) = 0$$

$$F_d(\xi, 0) = \omega\left(\frac{1-\xi}{2\xi}\right)^{1/2}\partial_\eta F_d(\xi, 0) \qquad G_d(\xi, 0) = 0 \qquad \partial_\eta Q_d(\xi, 0) = 0 \qquad \text{(5a–i)}$$

where ω is a particle-phase wall slip parameter. Equations (5a–d) indicate that far from the plate the two phases are in velocity equilibrium at the free stream speed and the particle-phase density is at its free stream value. Equations (5e, f) are the fluid-phase no slip conditions at the plate surface. Equations (5a–f) are the complete set of boundary conditions for the dusty-gas model. Equations (5g–i) are one of many plausible sets of surface conditions for the particle phase. In particular, Eq. (5g) allows for particle-phase wall slip in a manner similar to that used in rarefied gas dynamics. In reality, the particle-phase wall slip velocity is controlled by a variety of physical effects such as sliding friction, rolling friction, the nature of particle/surface collisions, particle shapes, etc. It is not possible to model such effects with precision at present, but by adjusting the slip parameter ω, it is, at least, possible to produce a wide variety of wall slip profiles. If particle-phase viscosity is omitted from the model it is no longer appropriate to impose particulate velocity boundary conditions at the plate surface. For this special case Eqs. (5g, h) should be dropped and Eqs. (3d, e) with ($\beta = 0$) should be solved at $\eta = 0$ as well as for $\eta > 0$. When evaluated at the wall, these equations can be solved in closed form (see Eq. (12)). One of the results is Eq. (5h) so, in reality, only Eq. (5g) needs to be dropped out for $\beta = 0$. If particle-phase diffusivity is omitted from the model, it is no longer appropriate to impose a particulate density boundary condition on the plate surface. For that reason Eq. (5i) is dropped out and Eq. (3c), with $\delta = 0$, is solved at $\eta = 0$ as well as for $\eta > 0$.

In the presentation of numerical result, reference will be made to the fluid and particle-phase skin-friction coefficients

$$C_c = \partial_\eta F_c(\xi, 0) \qquad \text{(6a)}$$

$$C_d = \beta\partial_\eta F_d(\xi, 0) \qquad \text{(6b)}$$

and to the fluid-phase displacement thickness coefficient

$$\Delta_c = \int_0^\infty (1 - F_c)d\eta \qquad \text{(7a)}$$

$$\Delta_d = \int_0^\infty (1 - F_d)d\eta \qquad \text{(7b)}$$

It can be seen from Eqs. (3) and (5) that at $\xi = 0$ (leading edge) the motions of the two phases are uncoupled (frozen flow). The fluid-phase solution is

$$F_c(0, \eta) = F_b(\eta) \qquad G_c(0, \eta) = G_b(\eta) \qquad \text{(8a, b)}$$

$$C_c(0) = C_b = F_b'(0) = \frac{a_1 + c_1\mathrm{Ha}_b + e_1\mathrm{Ha}_b^2 + g_1\mathrm{Ha}_b^3}{1 + b_1\mathrm{Ha}_b + d_1\mathrm{Ha}_b^2 + f_1\mathrm{Ha}_b^3} \qquad 0 \le \mathrm{Ha}_b \le 5.0$$

$$a_1 = 0.47587798 \qquad b_1 = 3.2544587 \qquad c_1 = 1.335379 \qquad d_1 = 3.9647233$$

$$e_1 = 4.7479162 \qquad f_1 = -0.0015819274 \qquad g_1 = 5.5774421 \tag{8c}$$

$$\Delta_c(0) = \Delta_b = \int_0^\infty (1 - F_b)d\eta = \frac{a_2 + c_2 \mathrm{Ha}_b + e_2 \mathrm{Ha}_b^2}{1 + b_2 \mathrm{Ha}_b + d_2 \mathrm{Ha}_b^2 + f_2 \mathrm{Ha}_b^3} \qquad 0 \le \mathrm{Ha}_b \le 5.0$$

$$a_2 = 1.2106207 \qquad b_2 = 1.7690139 \qquad c_2 = 2.2706381$$

$$d_2 = 3.2544861 \qquad e_2 = 0.78059673 \qquad f_2 = 1.099801 \tag{8d}$$

where F_b represent the modified Blasius solution in the presence of a magnetic field satisfying the problem

$$G_b' + F_d = 0 \qquad G_b F_b' = F_b'' - 2\mathrm{Ha}_b^2 (F_b - 1)$$

$$F_b(0) = 0 \qquad G_b(0) = 0 \qquad F_b(\eta) \to 1 \qquad \eta \to \infty \tag{9}$$

and Ha_b, is the Hartmann number for the modified Blasius solution. The errors for the correlations of C_d, and Δ_b in terms of Ha_b were found to be less than 0.1%. It should be noted that if Ha_b is equated to zero in these correlations, C_b, and Δ_b take on the respective values 0.476 and 1.211 which are close to the Blasius values.

In Eqs. (8) and (9), a prime denotes ordinary differentiation with respect to η. The corresponding particulate-phase solution is

$$F_d(0, \eta) = 1 \qquad G_d(0, \eta) = -\eta \qquad Q_d(0, \eta) = 1$$

$$C_d(0) = 0 \qquad \Delta_d(0) = 0 \tag{10}$$

It can be seen from Eqs. (3) and (5) that at $\xi = 1$ (far from leading edge) the motions of the two phases are identical (equilibrium flow). It can be shown (by solving Eq. (3a), the sum of Eqs. (3b) and (3d), and Eq. (3c) subject to Eqs. (5a, c, e, f, i) with all equations evaluated at $\xi = 1$) that Ha_1 is the Hartmann number for the solution at $\xi = 1.0$ and C_b, and Δ_b are evaluated from the correlations given in Eqs. (8) with $\mathrm{Ha}_b = \mathrm{Ha}_1/(1 + \kappa)^{1/2}$.

The physical interpretation of Eqs. (11) is that the equilibrium flow is the same as that associated with a single incompressible fluid having density $\rho_c + \rho_d = \rho_c(1 + \kappa)$ and dynamic viscosity $\mu_c + \mu_d = \mu_c (1 + \beta\kappa)$ (thus exhibiting kinematic viscosity $\nu_c (1 + \beta\kappa)/(1 + \kappa)$).

Solutions to Eqs. (3) were obtained numerically by an implicit finite difference method similar to that discussed by Blottner [18]. Constant step sizes in ξ and variable step sizes in η (with the smallest step adjacent to the plate) were employed. (The use of a variable step size in η was found to be especially helpful for $\beta = 0$.) All derivatives with respect to δ were represented by two-point backward-difference quotients. Derivatives with respect to η in Eqs. (3b–e) were represented by three-point central-difference quotients while η differencing of Eq. (3a) was accomplished by the trapezoidal rule. Two-point forward-difference quotients were used to represent the derivatives in Eqs. (5g, i). For the case of $\beta = 0$ boundary condition (5g) was replaced by Eq. (3d) evaluated at $\eta = 0$. For the case of $\delta = 0$ boundary condition (5i) was dropped and the η differencing of Eq. (3e) was carried out using the trapezoidal rule. The solution was started at $\xi = 0$ and marched downstream. On each line of constant ξ, iteration had to be used because of the nonlinear nature of the algebraic equations involved. Sets of linear tridiagonal algebraic equation were encountered at each stage of the iterative process. These were solved by the Thomas algorithm (see, for instance, Blott-

ner [18]). For the sake of brevity, further details of the numerical approach are omitted. In the next two sections a sampling of numerical results obtained using this procedure is presented and discussed. This sampling, though constituting only a small fraction of the predictions carried out in the course of the present work, is representative of the important trends observed.

Inviscid Particle Phase Solutions

Both Osiptsov [2] and Prabha and Jain [3] reported that, in the absence of a magnetic field, the particle-phase density became infinite at one relaxation length ($u_\infty\tau$) from the leading edge of the plate. For this reason, initial simulations were carried out for $\beta = 0$, $\delta = 0$, and Ha = 0 (dusty-gas model) and it was verified that the present numerical method also predicted this singular behavior. In all cases, the numerical results appeared to indicate the presence of a singularity of the particle-phase density at the plate surface located at $\xi = 0.5$ ($x = u_\infty\tau$). It was believed that the catastrophic growth in the particle-phase wall density at $\xi = 0.5$ is related to the vanishing of the particle-phase wall tangential velocity there. Inclusion of the magnetic field effects to the dusty-gas model did not alter the fact of existence of the singular behavior irregardless of the strength of the magnetic field. This is expected since the particle-phase tangential velocity at the wall remained unchanged regardless of the presence or absence of the magnetic field as will be shown subsequently.

A variety of simulations were performed for $\beta = 0$, $\delta \neq 0$ and Ha $\neq 0$. It was found that the inclusion of a particle-phase diffusivity eliminated the singularity discussed in the previous paragraph. While it was impossible to consider all values of δ, no value tested proved to be sufficiently small to preclude the existence of a continuous solution. The presence of the magnetic field for this case produced significant reductions in the particle-phase wall density. Some representative numerical results are shown in Figs. 2 to 8.

If Eqs. (3d, e) with $\beta = 0$ are evaluated at $\eta = 0$ it can be shown that they are satisfied by

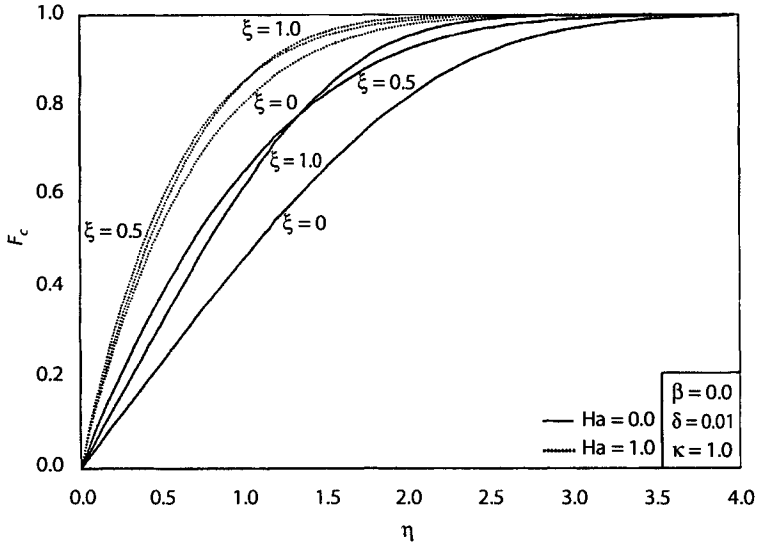

Fig. 2. Effects of Ha on fluid-phase tangential velocity profiles.

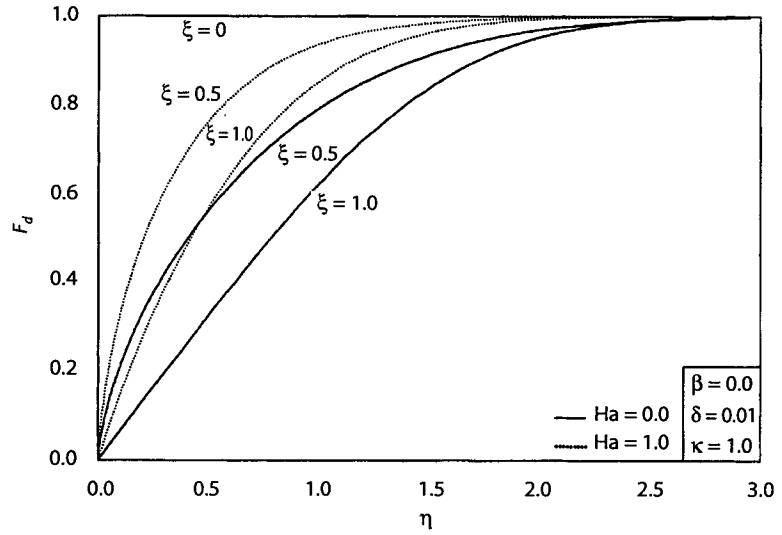

Fig. 3. Effects of Ha on particle-phase tangential velocity profiles.

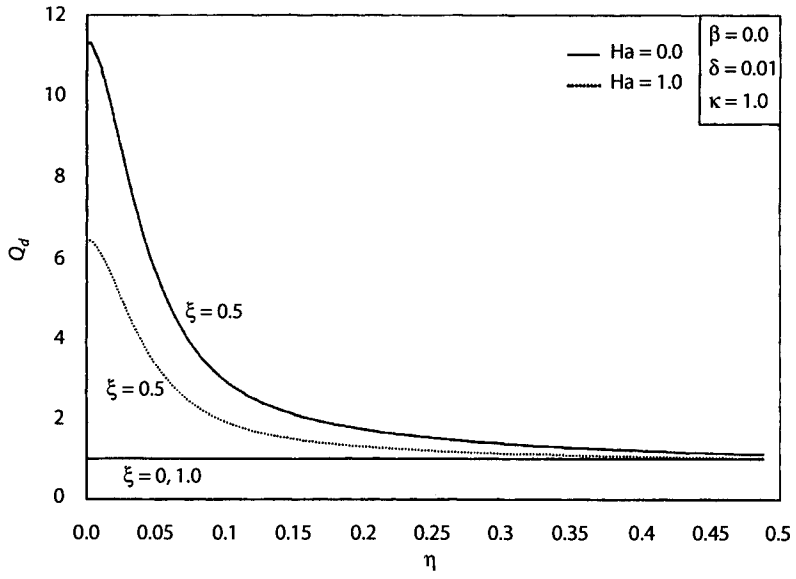

Fig. 4. Effects of Ha on particle-phase density profiles.

$$F_d(\xi, 0) = \begin{cases} \dfrac{1-2\xi}{1-\xi}; & 0 \le \xi \le 0.5 \\ 0 \;\; ; & 0.5 \le \xi \le 1 \end{cases}$$

$$G_d(\xi, 0) = 0 \qquad 0 \le \xi \le 1 \tag{11}$$

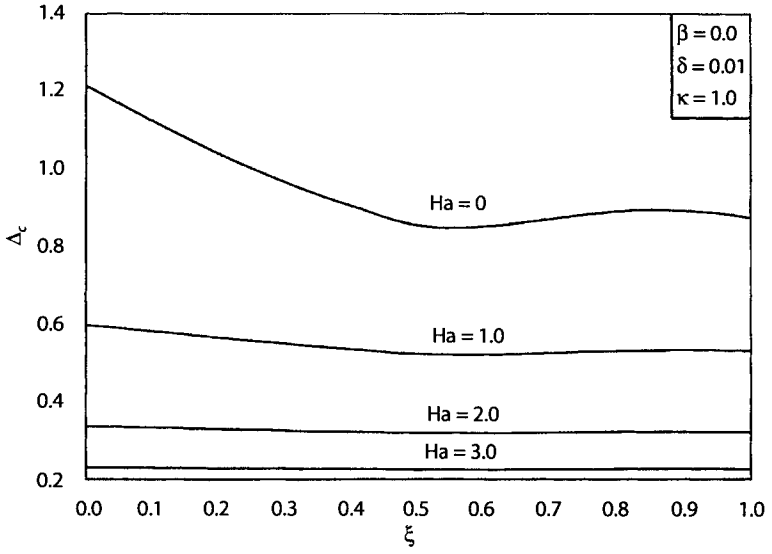

Fig. 5. Effects of Ha on fluid-phase displacement thickness.

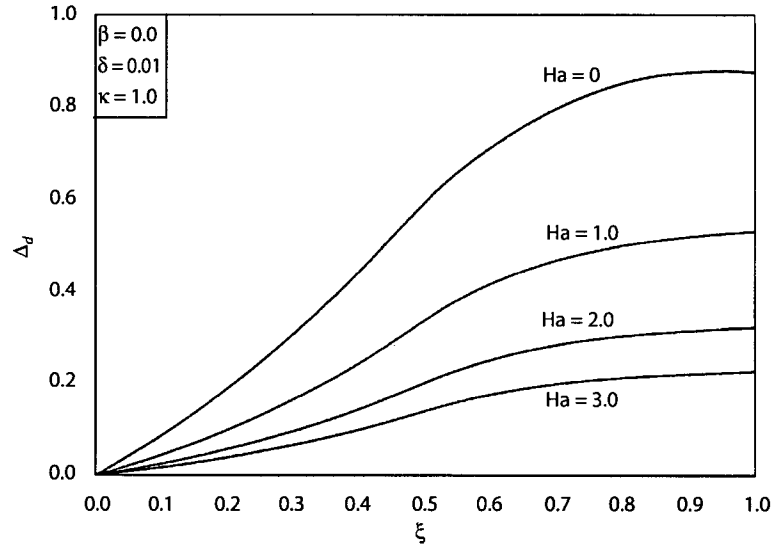

Fig. 6. Effects of Ha on particle-phase displacement thickness.

These results are independent of δ, κ, and Ha. Equations (11) show that the region $0.5 \leq \xi \leq 1$ on the plate surface is a stagnation line for the particle phase. Inspection of Eq. (1c) shows that for $D_d = 0$, ρ_d can not be finite at a particle-phase stagnation point. For $D_d \neq 0$, on the other hand, it can be. Thus, as mentioned above, the behavior of the particle-phase density predictions reported above is expected irregardless of the presence or absence of the magnetic field.

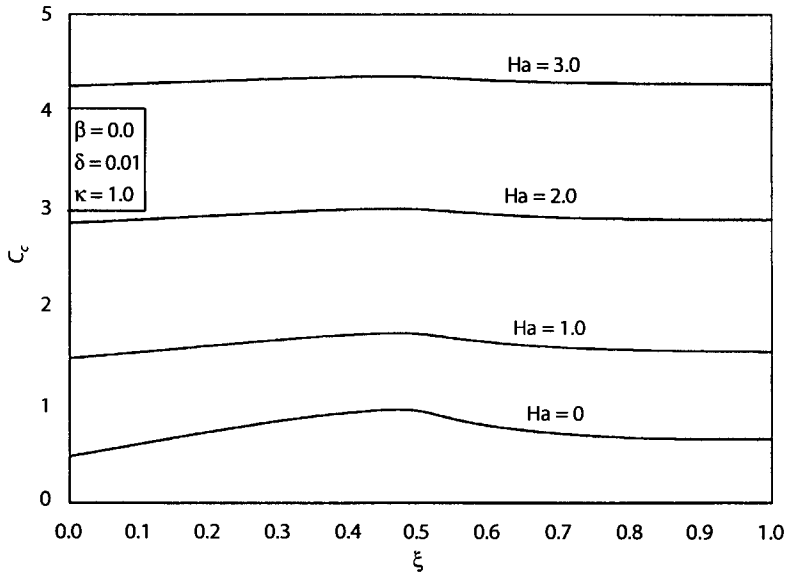

Fig. 7. Effects of Ha on fluid-phase skin-friction coefficient.

Figures 2 and 3 show typical tangential velocity profiles for the fluid and particulate phases, respectively, for $\kappa = 1.0$ and $\delta = 0.01$ at the two different values of Ha (Ha = 0 and Ha = 1.0). These figures illustrate the expected transition from frozen flow (no interphase momentum transfer) where both phases move independently at the leading edge to equilibrium flow (complete interphase momentum transfer) where both phases move together far down stream. The presence of the magnetic field is predicted to increase the fluid-phase tangential velocity at every ξ location. This is expected since the magnetic field term $-2\text{Ha}^2(F_c - 1)$ in Eq. (3b) acts as a motive force which acts in the direction of flow causing the fluid tangential velocity to increase. This increase in the fluid velocity is transferred to the particle phase through the interphase drag force causing the particle-phase tangential velocity to increase as well.

Figure 4 presents particle-phase density profiles computed at the same tangential locations and for the same parametric values associated with Figs. 2 and 3. It can be seen that the particle-phase density remains uniform at the free stream value over most of the boundary layer. Near the plate surface, its value first increases with tangential location reaching a maximum at $\xi = 0.5$ and then decreases back to unity at $\xi = 1.0$. The particle-phase density distribution is uniform both at the leading edge and far down stream. The increase in the particle-phase tangential velocity, mentioned before, as Ha increases causes its density to decrease as shown in Fig. 4.

Figures 5 and 6 show the fluid- and particle-phase displacement thicknesses Δ_c and Δ_d, respectively for $\delta = 0.001$, $\kappa = 1.0$ and various values of Ha. It can be seen that the fluid-phase displacement thickness undershoots its equilibrium value at $\xi = 1.0$ in some cases (Ha = 0 and Ha = 1.0) while the particle-phase displacement thickness increases with ξ until equilibrium between the phases is attained at $\xi = 1.0$. From the definition of Δ_c and Δ_d, it can be concluded that the increases in F_c and F_d as Ha increases cause both Δ_c and Δ_d to decrease. These behaviors are evident form Figs. 5 and 6.

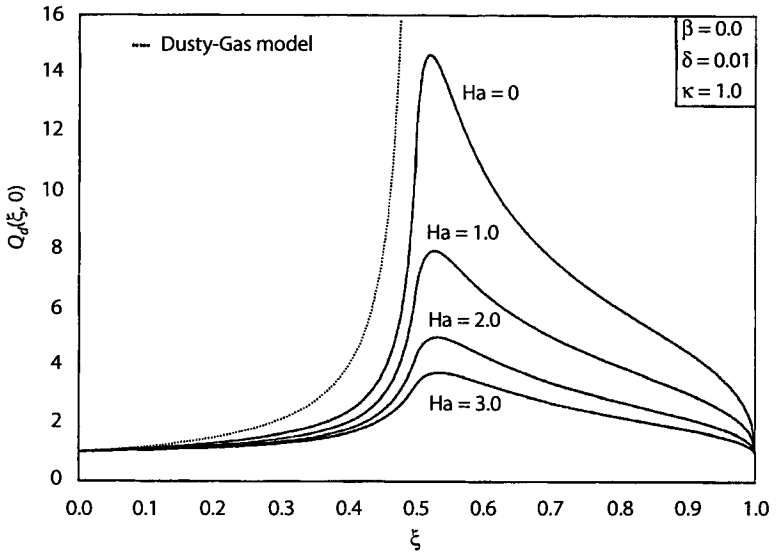

Fig. 8. Effects of Ha on particle-phase wall density.

Figure 7 illustrates the influence of the magnetic Hartmann number Ha on the fluid-phase skin-friction coefficient C_c for the same parametric conditions of Figs. 5 and 6. It can be seen that the skin-friction coefficient overshoots its equilibrium value at the same tangential location where Δ_c showed a corresponding undershoot. As seen from Fig. 2, the fluid-phase tangential velocity distribution increases as Ha increases causing its wall slope to increase. This has the direct effect of increasing the values of C_c as evident from Eq. (6a). These behaviors are depicted by the increases in C_c as Ha increases shown in Fig. 7.

Figure 8 reports the variation of the particle-phase density at the plate surface for the same parametric values employed to generate Figs. 5–7. It can be observed that $Q_d(\xi, 0)$ increases to a peak in the vicinity of $\xi = 0.5$ and then decreases. The peak becomes less pronounced as the strength of the magnetic field is increased. For $\delta = 0$ (dusty-gas model) the peaks are replaced by a rapid increase to infinity in the vicinity of $\xi = 0.5$ for all values of κ and Ha, as mentioned previously.

It is worth noting that other results not shown here for brevity showed that Δ_c was practically independent of the particle-phase diffusivity δ and that the dependence of C_c on this quantity was weak. In contrast, $Q_d(\xi, 0)$ exhibited a strong dependence on the particle-phase diffusivity δ. Reductions in δ produced large increases in the peak value.

Viscous Particle Phase Solutions

A number of simulations were carried out for various combinations of β, δ, κ, ω and Ha. The influence of particle-phase diffusivity was found to be qualitatively similar to that mentioned in the previous section. Continuous solutions were obtained only for $\delta \neq 0$. For the sake of brevity only one set of results is presented graphically herein. For this case the particle-phase diffusivity was fixed at $\delta = 0.1$, and the slip parameter was fixed at ($\omega = 0.001$. Some typical results associated with these parametric values are presented graphically in Figs. 9–13.

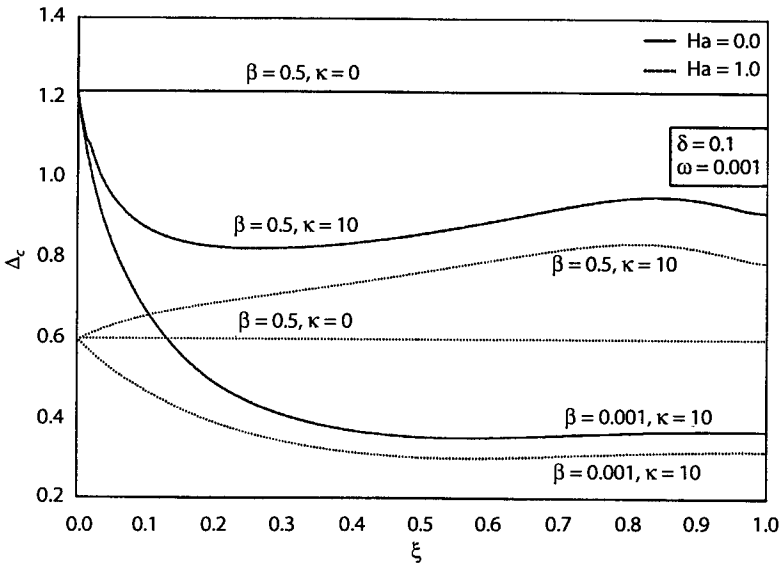

Fig. 9. Effects of β, κ and Ha on fluid-phase displacement thickness.

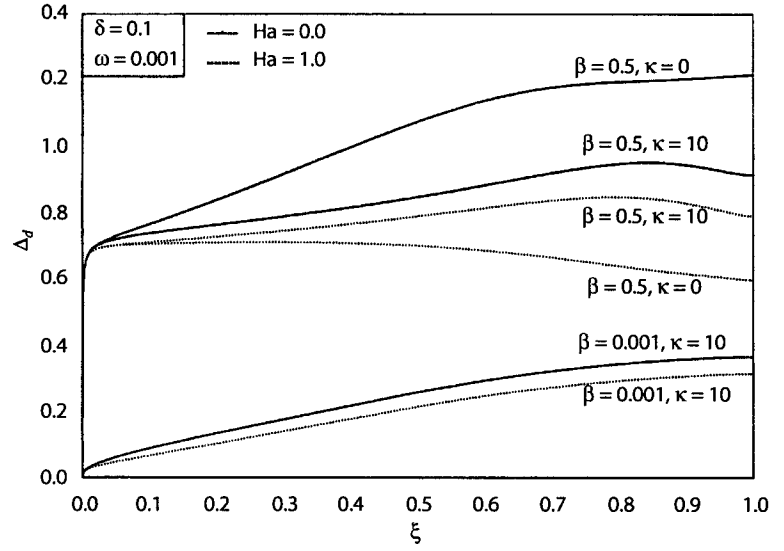

Fig. 10. Effects of β, κ and Ha on particle-phase displacement thickness.

For a non-vanishing value of β some representative tangential velocity profiles for the fluid and the particle phases were obtained that not shown here for brevity. It was observed from these profiles that equilibrium was reached rather quickly in this case because of the small value of the particle-phase wall slip parameter ω. For this small value of ω the particle phase obeys the no slip condition over virtually the entire plate surface. This was indicated by the fact that all the profiles except that associated with value of ω the particle phase obeys the no slip condition over virtually

the entire plate surface. This was indicated by the fact that all the profiles except that associated with $\xi = 0$ exhibited an absence of wall slip. Also, as Ha was increased, the tangential velocities of both phases increased.

Figures 9 and 10 display the fluid- and particle-phase displacement thicknesses, respectively, for two values of each of β, κ and Ha. In this parametric range, it is predicted that both Δ_c and Δ_d are increased as β is increased from 0.001 to 0.5. This is physically correct because increasing β increases the particle-phase viscous effects which cause reductions in the tangential velocities of both phases. This reduction in the tangential velocities produce higher displacement thicknesses. Figures 9 and 10 also show that as the particle loading κ is increased, both of Δ_c and Δ_d decrease in the absence of the magnetic field while they both increase in the presence of the magnetic field. This is interesting and is related to the fact that the effect of the external magnetic body force overcomes the influence of the drag force on the flow of the suspension. Physically, in the absence of the magnetic field, increasing κ causes the effective kinematic viscosity to decrease, therefore reducing the domain of influence of viscous effects. This results in decreases in Δ_c and increases in C_c. Also, as κ increases, the drag effect increases and thus, deviations from uniformity of the particle-phase tangential velocity profile occur. These become more pronounced as the distance from leading edge increases. Thus, Δ_d increases with ξ and decreases with κ for the reasons discussed above. However, in the presence of the magnetic field and for the parametric values used in Figs. 9 and 10, the magnetic motive force overcomes the drag force and the opposite behavior is predicted. In addition, these figures depict that increasing the magnetic Hartmann number Ha produces lower Δ_c and Δ_d values. This is consistent with what is discussed in the previous section.

The effects of β, κ and Ha on the fluid- and particle-phase skin-friction coefficients for the same parametric conditions used in Figs. 9 and 10 are illustrated in Figs. 11 and 12, respectively. When β is increased, C_c is predicted to decrease while C_d is predicted to increase (see Eq. (6b)). This decrease in C_c is due to the reduction in the wall slope of the fluid-phase tangential velocity

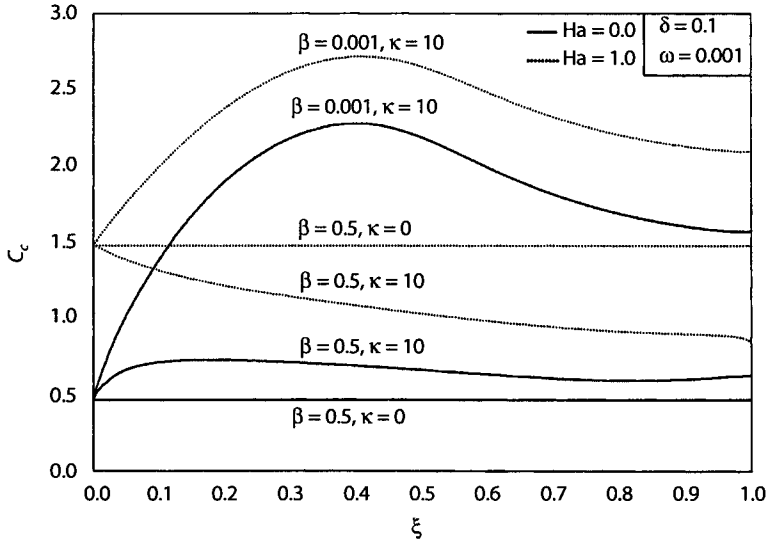

Fig. 11. Effects of β, κ and Ha on fluid-phase skin-friction coefficient.

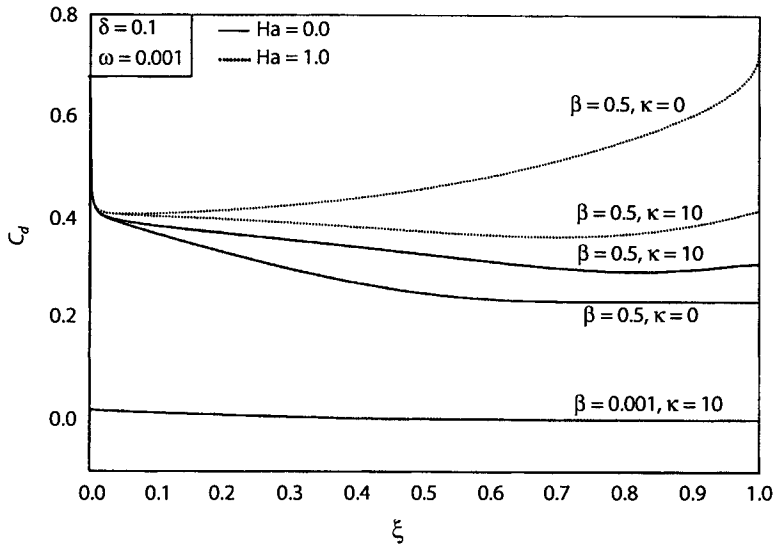

Fig. 12. Effects of β, κ and Ha on particle-phase skin-friction coefficient.

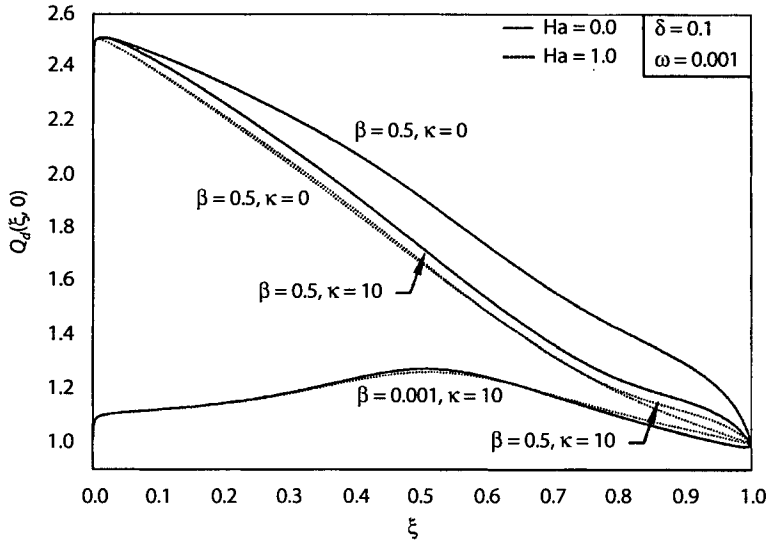

Fig. 13. Effects of β, κ and Ha on particle-phase wall density.

profile. For the physical reasons discussed in the previous paragraph and contrary to Δ_c and Δ_d, both C_c and C_d increase as κ increases for Ha = 0 while they both decrease as κ increases for Ha = 1. Again, both C_c and C_d are increased due to increases in the values of Ha for all β and κ combinations. It should be mentioned that all of the equilibrium result at $\xi = 1$ in Figs. 9–12 are consistent with the closed-form solutions reported earlier in Eqs. (11).

Figure 13 presents the particle-phase density variation at the plate surface for the same values of β, κ and Ha used to generate Figs. 9–12. For each curve corresponding to $\beta = 0.5$, a peak value of $Q_d(\xi, 0)$ exists near the leading edge of the plate and these peak values increase as the particle-phase diffusivity decreases as mentioned before. It is observed that as β increases, $Q_d(\xi, 0)$ increases everywhere in the range $0 < \xi < 1$. Increasing the particle loading is found to decrease the particle-phase wall density for the case where the magnetic field is absent. However, in the presence for the magnetic field, the values of $Q_d(\xi, 0)$ increased very slightly as κ is increased. This is in contrast with the results of Figs. 9–12. Similar to the inviscid particle-phase case ($\beta = 0$), $Q_d(\xi, 0)$ decreases as Ha increases.

As mentioned previously, the particle-phase obeys the no slip condition over almost the entire plate surface for the small value of ω used in these simulations. Larger values of ω increase the region in which particle-phase wall slip is significant and this, in turn, moves the location of the peaks in the particle-phase wall density profiles downstream.

Figure 9–13 contain results for the limiting case of $\kappa = 0$ (called the dilute limit by Soo [10] and [11]. In this limit, the fluid motion is unaffected by the presence of the particulate phase but the particulate motion is affected by the presence of the fluid phase (one way coupling). The dilute limit is obtained by formally equating the particle loading to zero but is intended to represent situations in which the particle loading is very small ($\kappa \ll 1$).

Conclusion

In the present paper, an extension of the dusty-gas model allowing for particle-phase diffusivity and viscosity was applied to the problem of plane, steady, laminar, boundary-layer flow of a fluid/particle suspension past a semi-infinite flat plate in the presence of a variable transverse magnetic field. Solutions were obtained numerically by a standard finite-difference technique. Four points of interest illustrated by these solutions are discussed below.

First, the results presented herein show that physically plausible changes in fluid/particle suspension models can lead to significant qualitative (not just quantitative) changes in predictions. This makes clear the need for pertinent experimental data which can be used for model verification. The present authors were unable to locate any experimental work in the literature dealing with laminar boundary-layer flow of a particulate suspension past a flat plate in the presence of a magnetic field.

Second, it is interesting that the influence of particulate diffusivity was confined almost entirely to the particulate density predictions. Very little influence of the particulate diffusivity on the other flow variable was observed.

Third, in the presence of a particulate diffusivity, the applied magnetic field had a marked influence on the maximum value attained by the particle-phase wall density. In addition, the displacement thicknesses of both phases increased and their skin-friction coefficients decreased as the particle loading was increased. This was in contrast with the case where the magnetic field was absent in which the displacement thicknesses decreased and the skin-friction coefficients increased as the particle loading was increased.

Fourth, solutions of the title problem based on the dusty-gas model are not self consistent. This is because the prediction of an infinite particle-phase density in the presence or absence of the magnetic field violates the small volume fraction assumption on which the model is based. The predictions of the model employed herein, on the other hand, are self consistent. That suggests that models of this general type should receive greater attention in the future.

REFERENCES

1. Cramer, K. R. and Pai, S.-L., *Magnetofluid Dynamics for Engineers and Applied Physicists*, Scripta Publishing Company, Washington, D.C., 1973.
2. Osiptsov, A. N., Structure of the Laminar Boundary Layer of a Disperse Medium on a Flat Plate, *Fluid Dyn.*, 1980, **15**, pp. 512–517.
3. Prabha, S. and Jain, A. C., On the Use of Compatibility Conditions in the Solution of Gas Particulate Boundary Layer Equations, *Appl. Sci. Res.*, 1980, **36**, pp. 81–91.
4. Wang, B. Y. and Glass, I. I., Compressible Laminar Boundary-Layer Flows of a Dusty Gas Over a Semi-Infinite Flat Plate, *J. Fluid Mech.*, 1988, **186**, pp. 223–241.
5. Chamkha, A. J. and Peddieson, J., Boundary Layer Theory of a Particulate Suspension with Finite Volume Fraction, *ASME Journal of Fluids Engineering*, 1994, **116**, pp. 147–153.
6. Chamkha, A. J., Compressible Dusty-Gas Boundary-Layer Flow over a Flat Surface, *ASME Journal of Fluids Engineering*, 1996, **118**, pp. 179–185.
7. Chamkha, A. J., Effect of Combined Particle-Phase Diffusivity and Viscosity on the Compressible Boundary Layer of a Particulate Suspension over a Flat Surface, *ASME Journal of Heat Transfer*, 2000.
8. Marble, F. E., Dynamics of Dusty Gases, *Ann. Rev. Fluid Mech.*, 1970, **2**, pp. 397–446.
9. Rosso, V. J., On Flow of Electrically Conducting Fluids over a Flat Plate in the Presence of a Transverse Magnetic Fields, *NACA Report*, 1958, p. 1358.
10. Soo, S. L., Fluid Dynamics of Multiphase Systems, *Blaisdell Publishing Company*, 1967, pp. 324–341.
11. Soo, S. L., Non-Equilibrium Fluid Dynamics-Laminar Flow over a Flat Plate, *ZAMP*, 1968, **19**, pp. 545–563.
12. Soo, S. L., Development of Theories on Liquid-Solid Flows, *J. Pipelines*, 1984, **4**, pp. 137–142.
13. Korjack, T. A. and Chen, R. Y., Deposition of Suspensions in the Entrance of a Parallel-Plate Channel with Gravity Effect, *Comptrs. Fluids*, 1980, **8**, pp. 305–311.
14. Chiam, T. C., Hydromagnetic Flow over a Surface Stretching with a Power-Law Velocity, *Int. J. Engng. Sci.*, 1995, **33**, pp. 429–435.
15. Buyevich, Y. A., Statistical Hydromechanics of Disperse Systems Part 1 – Physical Background and General Equations, *J. Fluid Mech.*, 1971, **49**, pp. 489–507.
16. Drew, D. A., Averaged Field Equations for Two-Phase Media, *Studies Appl. Math.*, 1971, **50**, pp. 133–166.
17. Ungarish, M. and Greespan, H. P., On Two-Phase Flow in a Rotating Boundary Layer, *Studies Appl. Math.*, 1983, **69**, pp. 145–175.
18. Blottner, F. G., Finite Difference Methods of Solution of the Boundary Layer Equations, *AIAA J.*, 1970, **8**, pp. 193–205.

□◆◆◆□